Open Veterinary Journal, (2023), Vol. 13(6): 723-731
ISSN: 2226-4485 (Print)
ISSN: 2218-6050 (Online)
Original Research
DOI: *10.5455/OVJ.2023.v13.i6.7*

Submitted: 19/03/2023 Accepted: 09/05/2023 Published: 09/06/2023

Nephrotoxicity induced by different diameters of sphere gold nanoparticles with special emphasis on the nephroprotective role of quercetin

Foll-Alnada A. F. Abdelrahman, Shafika A. El-Sayed, Ahmad A. Abuel-Atta and Wael A. M. Ghonimi*

Department of Histology and Cytology, Faculty of Veterinary Medicine, Zagazig University, Zagazig, Egypt

Abstract

Background: Although, gold nanoparticles (GNPs) are attracting more and more attention due to their ease of synthesis, modification, and great potential value in biomedical applications, exhibited harmful effects on human health and other living species. Quercetin (Qur) clarifies diverse pharmacological effects, especially anti-inflammatory, antiapoptotic, and antioxidant ones.

Aim: This study aimed to evaluate the probable nephrotoxicity induced by different diameters of sphere GNPs, as well as the nephroprotective role of Qur.

Methods: A total of 54 healthy mature male albino rats were grouped and treated with or without sphere GNPs; 10, 20, and 50 nm and Qur (200 mg/kg b.wt.). The effects of GNPs and Qur were estimated through the collection of blood and kidney samples from euthanized rats and performed biochemical, histopathological, and immunohistochemical investigations.

Results: In comparison between different diameters of GNPs, the 10 nm GNPs revealed more significant elevations in all renal function parameters: creatinine, urea, blood urea nitrogen, and uric acid followed by 20 nm then 50 nm. Pre-cotreatment with Qur decreased all renal functional values. Histopathologically, 10 nm revealed the most potent renal pathological changes represented in the renal cortex with cloudy swelling of renal tubules, hypercellularity of some glomeruli, severe congestion of renal blood vessels, focal inter tubular edema, and vascular endotheliosis (degeneration of endothelium). In addition, the renal medulla revealed perivascular inflammatory cellular infiltration, perivascular fibrosis, intra tubular glycogen deposition, and casts deposition of mainly cellular casts. On the other hand, the Qur treatment ameliorated most of these pathological changes.

Conclusion: The size of GNPs is pivotal in their pathological effect on renal tissues where the small-sized GNPs; 10 nm have more potent cytotoxic, inflammatory, and apoptotic effects rather than the larger ones. Otherwise, Qur clarified a significant mitigating role against the nephrotoxicity of the GNPs.

Keywords: Gold nanoparticles, Nephrotoxicity, Quercetin, GNPs, Nephroprotective.

Introduction

Nanoparticles (NPs) are highly precise chemical and physical features that have multiple potential uses in nano-biomedical technology. Their target and body-wide circulation can be affected by their physical properties, and they can be delivered in NPs or coupled with therapeutic drugs for precise, controlled delivery to target tissues. Additionally, NPs of all sizes can cause oxidative stress and free radical formation, which can injure tissues, cells, and macromolecules (Abdelhalim and Jarrar, 2011, 2012; Jeevanandam *et al*., 2018; Bayda *et al*., 2019; Gheorghe *et al*., 2021).

Gold NPs (GNPs) are one from the family of metallic NPs and are divided into multi subtypes, such as nanospheres, nanocages, nanorods, and nanoshells (Cai *et al*., 2008). They have been explored for optical sensors, imaging, drug administration, and therapeutic applications due to their size, structure, physical properties, and intrinsic biocompatibility (Falagan *et al*., 2016; Jiang *et al*., 2016; Kong *et al*., 2017; Xu *et al*., 2017).

GNPs are a promising biomedical application due to their high stability and biocompatibility with a wide range of chemicals and biological components, enabling the manufacture, analysis, and combination of a variety of diagnostic, therapeutic, and delivery systems (Wang *et al*., 2012; Chen *et al*., 2013; Kumar *et al*., 2013).

For many decades, gold has been employed in therapeutic techniques, including Chinese and Indian treatments. They were mostly used to treat arthritic conditions. However, it was eventually shown that extended exposure to gold induced nephrotoxicity. As a result, they were restricted in medical practice (Yamashita, 2021).

Quercetin (Qur) is a flavonoid found in the human diet that has significant pharmacological effects. Its IUPAC

***Corresponding Author:** Wael A. M. Ghonimi. Department of Histology and Cytology, Faculty of Veterinary Medicine, Zagazig University, Zagazig, Egypt. Email: *ghonimi102030@gmail.com; waghonimi@zu.edu.eg*

designation is (3,5,7,3,4, pentahydroxy flavone). It has a yellow crystalline solid shape, with a bitter taste, soluble in alcohol, glacial acetic acid, alkaline aqueous solutions, and water. It is found in broccoli, lettuce, apples, tomatoes, onions, tea nuts, seeds, stems, blossoms, roots, bark, and coffee (Jellin *et al*., 2003; Baghel *et al*., 2012).

Qur is a natural antioxidant element with antiviral, pro-metabolic, and anti-inflammatory activities. It is effective as a cancer-prevention agent and has been proven to reduce platelet aggregation, capillary permeability, and lipid peroxidation while increasing mitochondrial biogenesis (Aguirre *et al*., 2011; Dabeek and Marra, 2019).

Due to its wide range of health advantages, Qur is gaining traction and is a key ingredient in the creation of innovative and potent functional foods and medications. One of the pharmacological effects is antioxidant activity (Hatahet *et al*., 2017; Yang *et al*., 2018). Qur reduces the spread of cancers, such as lung, prostate, liver, breast, colon, and cervical cancer. Its anticancer properties are mediated by a number of mechanisms, including cell signaling pathways and enzyme activity that block carcinogens (Xu *et al*., 2019).

The present investigation aimed to evaluate the possible nephrotoxicity induced after the intraperitoneal injections of different diameters of sphere GNPs; 10, 20, and 50 nm with special reference to the possible nephroprotective effect of Qur against the renal toxicity of GNPs.

Materials and Methods

Animals and housing

The present study was performed on 54 mature male albino rats purchased from the Laboratory Animal Unite at Veterinary Medicine Faculty, Zagazig University, Egypt. The animals weighed 180 ± 20 g and were housed in a controlled room with suitable conditions such as 14 hours of light and 10 hours of dark cycle and normal temperature (20°C–23°C). Rats were kept in transparent polypropylene cages where food and water were available *ad libitum*. Rats were acclimatized for 1 week in the laboratory before the beginning of the experiment to avoid transportation stress.

Supplements

Gold NPs

Different diameters of sphere GNPs; 10, 20, 50 nm were utilized in this study in an aqueous solution at a concentration of 0.01% with pH 8, molecular weight 196.97, density 19.32 g/cm^3, and specific surface area 3.394 m^2/g. GNPS were purchased from Nano Gate Company, Egypt.

Quercetin

Qur was also purchased from Nano Gate Company, Egypt, in the form of yellow powder with molecular weight 302.24 g/mol (anhydrous basis) and purity of 95% by high-performance liquid chromatography. An aqueous solution of Qur was prepared for a dose of 200 mg/kg bw per day on water for suspension.

Experimental design

Fifty-four mature male albino rats were grouped randomly (n = 9 rats/group) for two studies, the first study is to clarify the possible nephrotoxicity induced by different diameters of GNPs, such as 10, 20, 50 nm for 7 days. Then, the biochemical and histopathological toxicity of GNPs was evaluated after 1 week from the end of the first study to detect the most toxic diameter of GNPs. Furthermore, the second study was begun to evaluate the nephroprotective role of Qur against the most toxic diameter of GNPs.

The first study (acute toxicity study of GNPs)

Animals were divided into four groups (n= 9 rats/group) and subjected to one of the following treatments for 7 days:

Group I (G1, control group), rats were only fed with a basal diet without any treatment for 7 days.

Group II (G2), III (G3), and IV (G4), rats were intraperitoneally injected with 10, 20, and 50 nm diameter of sphere GNPs, respectively, in a dose of 75 µg/kg bw of rat, once a day for 7 days according to Orabi *et al*. (2022).

After 48 hours, animals were euthanized then, kidney samples were collected and utilized for histopathological investigation, and serum blood samples were collected for biochemical investigation.

The second study (protective study of Qur)

Animals were subjected for 14 days to one of the following treatments:

Group V (G5), animals were only given Qur orally once a day for 14 days in a dose 200 mg/kg bw according to Abdelhalim *et al*. (2018).

Group VI (G6), animals were orally treated with Qur for 14 days with the same previous dose but at the last 7 days from 14 days, animals were co-treated with both Qur and 10 nm diameter (most toxic diameter detected from the first study) of sphere GNPs intraperitoneally in a dose 75 µg/kg bw.

Blood sampling

After 24 hours of the final dose injection, all animals were fasted for 12–14 hours before being euthanized, and thereafter, 54 blood samples were collected into sterilized tubes without anticoagulant for serum separation. Centrifugation was carried out at 3,000 rpm for 10 minutes to separate the serum, then, the serum was conserved at a temperature of −80°C for biochemical assessments.

Serum biochemical analysis

To evaluate the renal function, the levels of creatinine, urea, uric acid, and blood urea nitrogen (BUN) were measured for 54 samples.

Histological and histochemical processing

At the end of the experiment, the cervical dislocation of animals was carried out and kidneys were separated for histological examination and fixed in Bouin's solution, then transferred to neutral buffered formalin 10% for 48 hours. The specimens were processed histologically, dehydrated in ascending grades of ethanol, cleared in

xylene, and embedded in melted paraffin wax forming paraffin blocks. 4–5 µm thick sections were obtained and stained with Harris' hematoxylin and eosin (H & E), Perl's Prussian blue reaction, periodic acid-Schiff (PAS), and blue Masson's Trichrome according to Suvarna *et al*. (2018).

Immunohistochemical investigation

Immunohistochemical staining was performed on 5 µm, formalin-fixed, paraffin-embedded sections using anti-caspase-3 (ab184787), rabbit monoclonal primary antibodies as a marker of apoptosis at a dilution 1:1,000, through the streptavidin-biotin technique. Deparaffinized sections were stained by an indirect immunoperoxidase technique (Polak and Noorden, 1997). The stained sections were photographed by a digital camera (Canon) connected to a light microscope (Zeiss).

Statistical analysis

Results were clarified as mean ± standard error of mean. To evaluate the impact of the six treatment groups on the various biochemical parameters, one-way analysis of variance by Fisher tests as *post hoc* tests were utilized. The $p < 0.05$ value was utilized to signalize the statistical significance. All analyses and charts were performed using Statistical Package for Social Sciences version 28.0 (SPSS, IBM Corp., Armonk, NY) and Graph Pad Prism 8.0.2 (GraphPad Software, Inc).

Ethical approval

The research protocol has been reviewed and approved by the Institutional Animal Care and Use Committee, Zagazig University, Egypt, with an approval number (ZU—IACUC; No. ZU-IACUC/2/F/250/2022).

Results

Biochemical analysis (renal function parameters)

All tested renal function parameters, such as serum creatinine, urea, BUN, and uric acid clarified a significant elevation in all treated groups with different diameters of GNPs; 10, 20, and 50 nm but, the G2 injected with 10 nm was the most affected group and recorded the most increase for all renal parameter values followed by G3 injected with 20 nm and then G4 injected with 50 nm GNPs. Meanwhile, G5 (Qur only) recorded values near the control group. In addition, G6 (Qur and 10 nm GNPs) showed a good impact and recorded a significant decrease in all values compared to G2 (Fig. 1).

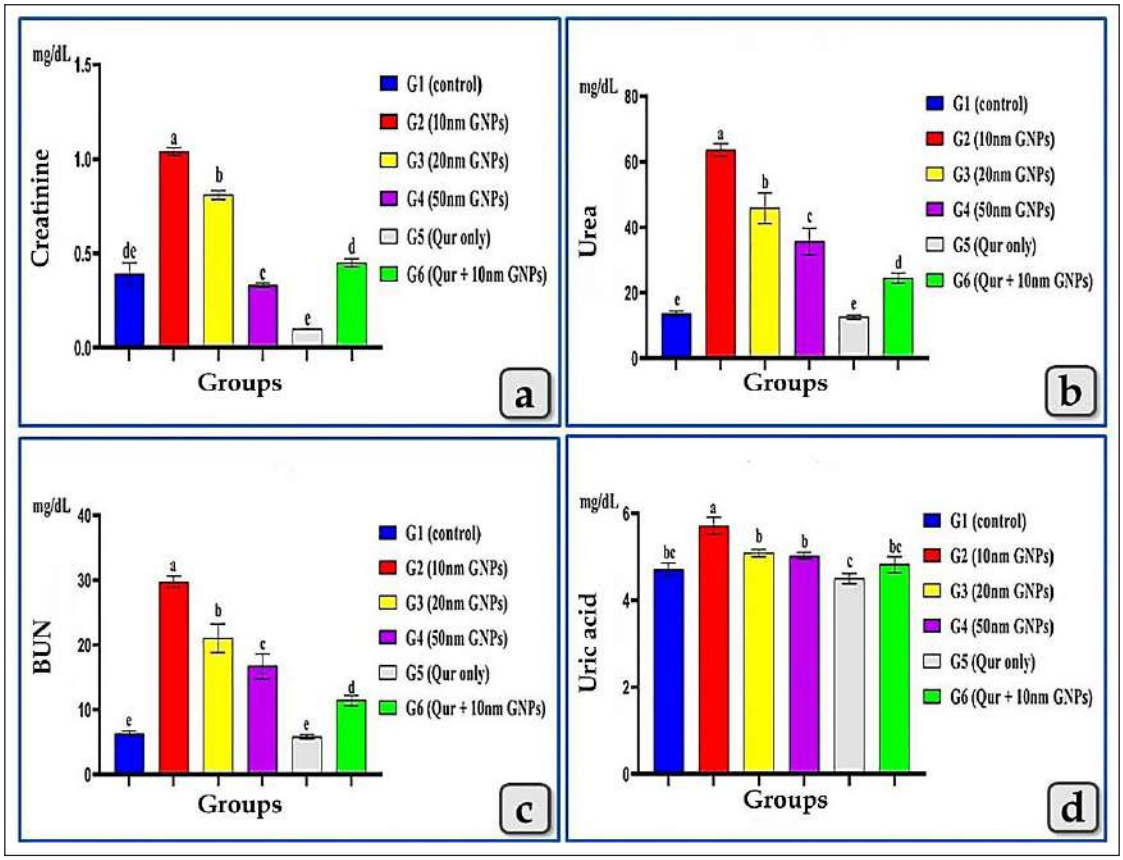

Fig. 1. Showing the effect of different diameters of GNPs and Qur on some renal functional parameters; creatinine, urea, BUN, and uric acid levels for all experimental groups. According to the Fisher test, the different letters (a–e) are significantly different between treatments at the $p < 0.05$ level.

Histopathological analysis

The kidney of G1 (control group) revealed normal, intact renal cortex and medulla without any abnormalities (Fig. 2a and b). Meanwhile, G2 injected with 10 nm GNPs clarified the most potent histopathological changes in the renal cortex and medulla. Whereas, the renal cortex was characterized with cloudy swelling of renal tubules at which renal epithelium bulged into lumen and became star-like shape and severe intertubular hemorrhage (Fig. 2c), with focal intertubular edema (Fig. 2d). Also, vascular endotheliosis (degeneration of endothelium) was detected with perivascular edema (Fig. 2e). In addition, sever intra and intertubular glycogen depositions were detected by PAS stain and stained with deep magenta coloration (Fig. 2f). Sever vascular endotheliosis and vacuolations of vascular tunica media were demonstrated (Fig. 2g). But, the renal medulla of G2 revealed sever hemorrhage with perivascular inflammatory cellular infiltration (Fig. 2h), perivascular fibrosis represented in accumulation of collagen fibers that was demonstrated by Blue Masson's Trichrome stain (Fig. 2i). Furthermore, intratubular diffused glycogen depositions were demonstrated by PAS stain (Fig. 3a), and few cases showed renal medulla with intratubular casts depositions of mainly cellular casts (Fig. 3b). In addition, some cases showed both hypercellularity of some glomeruli with cloudy swelling of the renal tubules lining epithelium (Fig. 3c). While G3 injected with 20 nm GNPs demonstrated moderate atrophy of some renal tubules, intertubular edema and cystic dilation of others (Fig. 3d), individualization of some renal tubules in the renal cortex (Fig. 3e), and focal hemosiderosis in renal medulla (Fig. 3f). Moreover, G4 injected with 50 nm GNPs showed mild congestion of renal blood vessels with perivascular inflammatory cells infiltration in the renal cortex (Fig. 3g), with focal hypercellularity of few glomeruli with focal cloudy swelling of some renal epithelium (Fig. 3h), and mild atrophy of some renal glomeruli (Fig. 3i). But, the renal medulla of G4 clarified a focal area of cystic dilation of some renal tubules with edema (Fig. 4a and b), apoptosis of some renal epithelium and cloudy swelling of renal tubules (Fig. 4c). Furthermore, G5 (Qur only) revealed normal,

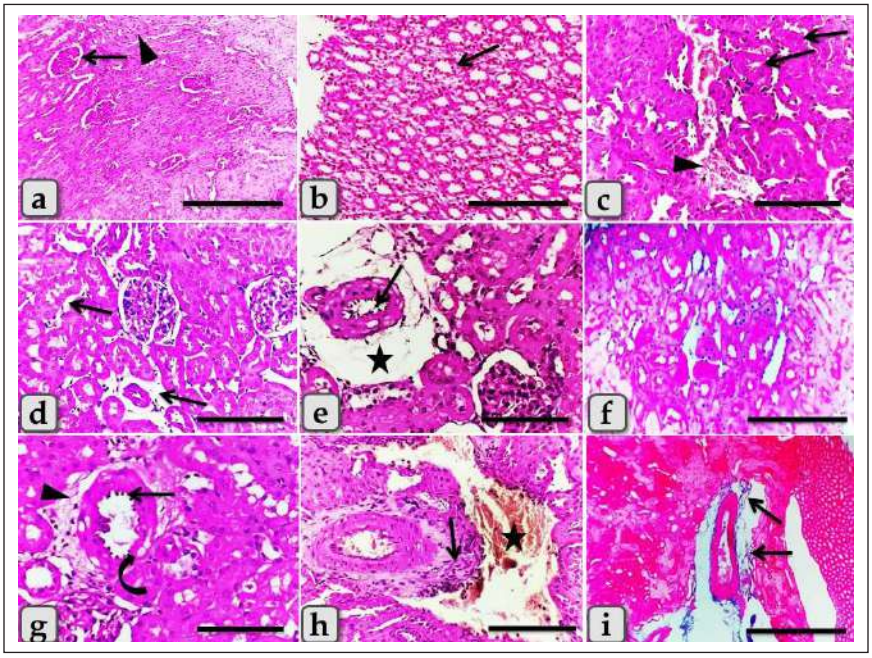

Fig. 2. Photomicrographs of the kidney of G1, control group (a and b), and G2 (c–i) that were injected intraperitoneally with 10 nm GNPs for 7 days showing, (a) normal renal cortex with normal glomeruli (arrow) and intact renal tubules (arrowhead). (b) Normal renal medulla with normal renal tubules (arrow). (c) Renal cortex with cloudy swelling of renal tubules (arrow) and severe intertubular hemorrhage (arrowhead). (d) Renal cortex with focal intertubular edema (arrows). (e) Renal cortex with vascular endotheliosis (arrow) and perivascular edema (star). (f) Intra and intertubular glycogen depositions. (g) Renal cortex with perivascular edema (arrowhead), vascular endotheliosis (arrow), and vacuolations of tunica media (curved arrow). (h) Renal medulla with severe hemorrhage (star) and perivascular inflammatory cellular infiltration (arrow). (i) Renal medulla with perivascular fibrosis represented in accumulation of collagen fiber (arrows). Stain: (all) H & E, except, (f) PAS, (i) Blue Masson trichrome. Scale bars: All = 600 µm except, (c, d, e, g, and h) = 200 µm.

intact renal tissues that appeared looks like the control group in the renal cortex (Fig. 4d) and medulla (Fig. 4e). Moreover, G6 (Qur + 10 nm GNPs) showed normal renal cortex but with slight hypercellularity of some renal epithelium (Fig. 4f), with normal renal tubules (Fig. 4g), and mild intratubular glycogen deposits (Fig. 4h), while the renal medulla of G6 clarified mild focal cystic dilation of some renal tubules (Fig. 4i). In addition, semi-quantitative histopathological lesion scores for all experimental groups were recorded in Table 1.

The immunohistochemical reactivity of the kidney against the anti-caspase-3 antibody for all experimental groups clarified negative expression for caspase-3 (Fig. 5a and e) for both G1 and G5, respectively. Distributions of the strongly positive expression with severe peripheral expressions for caspase-3 in G2 were observed (Fig. 5b). Moderate to strong positive expressions were scattered randomly in G3 (Fig. 5c). Focal mild positive expression in G4 was demonstrated (Fig. 5d). Limited mild to moderate positive cellular expressions for caspase-3 in G6 were clarified (Fig. 5f).

Discussion

The current study clarified a significant elevation in all tested renal functional parameters, such as creatinine, urea, uric acid, and BUN after the administration of different diameters of sphere GNPs but G2 injected with 10 nm GNPs recorded the highest values followed by G3 (20 nm GNPs), then G4 (50 nm GNPs). These results indicated that the smaller diameters of GNPs induce a potential change in the tested renal functional parameters more than the larger ones. These findings are supported by the findings of Abdelhalim *et al*. (2020) who clarified that GNPs cause an elevation in BUN levels in comparison to the treated group and with Doudi and Setorki (2014) who elucidated that the levels of creatinine, BUN, and uric acid were elevated in all groups treated with GNPs when compared with the control group.

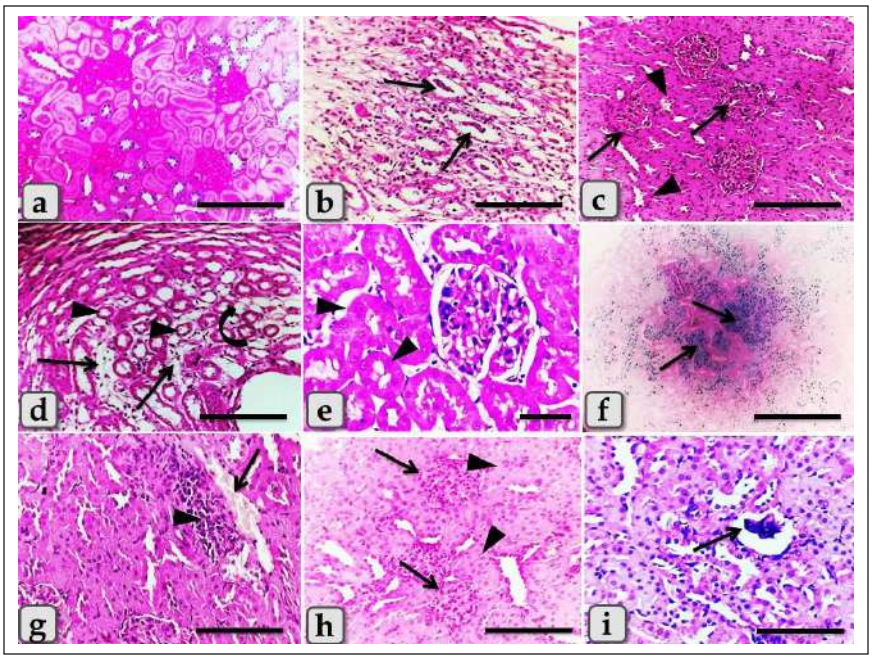

Fig. 3. Photomicrographs of the kidney of G2 (a–c), G.3 (d–f), and G4 (g–i) that were injected intraperitoneally with 10, 20, and 50 nm GNPs, respectively, for 7 days showing, (a) renal medulla with intratubular diffused glycogen deposition. (b) Renal medulla with intra tubular casts deposition (arrows) of mainly cellular casts. (c) Hypercellularity of some glomeruli (arrows) with degeneration of some renal tubules represented in cloudy swelling of the renal epithelium (arrows head). (d) Renal medulla with atrophy of some renal tubules (arrows head), inter tubular edema (arrows), and cystic dilation of others (curved arrow). (e) Renal cortex with individualization of some renal tubules (arrows head). (f) Renal medulla with focal hemosiderosis (arrows). (g) Renal cortex with congestion of renal blood vessels (arrow) with perivascular inflammatory cell infiltration (arrowhead). (h) Renal cortex with focal hypercellularity of few glomeruli (arrows) with focal cloudy swelling of some renal epithelium (arrow head). (i) Renal cortex with atrophy of some renal glomeruli (arrow). Stain: (all) H & E, except, (a) PAS, (f) Perls Prussian blue. Scale bars: All = 200 µm except, (e) = 30 µm.

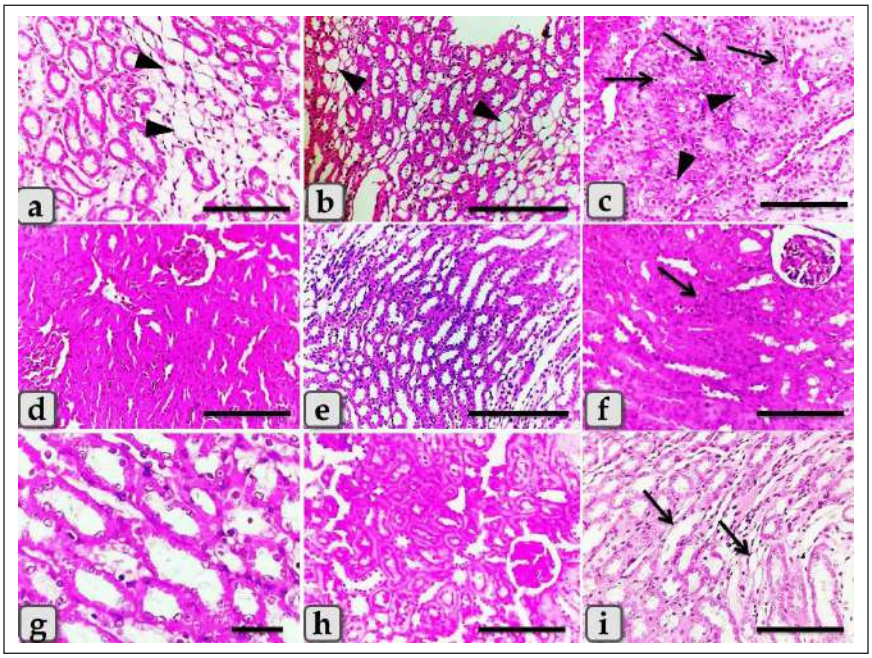

Fig. 4. Photomicrographs of the kidney of G4 (a–c) that injected intraperitoneally with 50 nm GNPs, G5 (d–e) treated with Qur, and G6 (f–i) that treated with Qur and injected intraperitoneally with 10 nm GNPs showing, (a and b) Renal medulla with a focal area of cystic dilation of renal tubules (arrow heads) and edema. (c) Renal medulla with apoptosis of some renal epithelium (arrows) and cloudy swelling of renal tubules (arrows head). (d) Renal cortex with apparently normal renal glomeruli and renal tubules. (e) Renal medulla with apparently normal renal tubules. (f) Renal cortex with normal renal glomeruli and renal tubules but with slight hypercellularity of some renal epithelium (arrow). (g) Renal cortex with normal renal tubules and normal lining epithelium. (h) Renal cortex with mild intratubular glycogen deposits. (i) Renal medulla with mild cystic dilation of some renal tubules (arrows). Stain: (all) H & E. except (h) PAS. Scale bars: All = 200 µm except, (b and e) = 600 µm and (g) = 30 µm.

Meanwhile, G5 (Qur only) recorded values near to the control group. In addition, G6 (Qur and 10 nm GNPs) showed a good impact and recorded a significant decrease in all values compared to G2. These results indicated the protective efficacy of Qur in the improvement of renal functional parameters when given with 10 nm GNPs. These findings were supported by Alasmari (2021) who assumed that Qur provided protection against a variety of chemicals and toxins by serving as antioxidants, regulating renal enzymes, strengthening antioxidant defense mechanisms, and decreasing apoptosis-mediated toxicities in Wistar male rats injected intraperitoneally with 50 µl of 10 nm GNPs for 7 days.

Severe histopathological changes were clarified in G2 injected with 10 nm GNPs as cloudy swelling of renal tubules, focal intertubular edema, severe congestion of renal blood vessels, degeneration of endothelium, intratubular casts, and perivascular inflammatory cellular infiltration. These results were supported by Jarrar and Alferah (2014) and Ibrahim *et al*. (2018) who revealed that 10 nm GNP exposures caused pathological alterations in rats, including edema, hydropic degeneration, and hyaline casts. In addition, karyorrhexis, karyolysis, pyknosis, and apoptosis were reported in some renal cells after 10 days of GNPs exposure.

Furthermore, resembling other metal oxide NPs, we observed several renal histopathological changes induced after the injection of GNPs that were typically similar to that described after the injection of copper oxide NPs as atrophy of renal glomeruli, cloudy swelling of the renal tubules, intertubular hemorrhage, diffuse inflammatory cells infiltrations and perivascular fibrosis (Ghonimi *et al*., 2022).

G3 injected with 20 nm GNPs clarified moderate atrophy of some renal tubules, moderate intertubular edema, and cystic dilation of others. This finding goes hand in hand with the finding of Fadia *et al*. (2022) who found massive congestive vessels, numerous lymphocyte infiltrations, tubular degeneration, and a necrotic condition in the 20 nm GNPs treated rat kidneys. However, G4 injected with 50 nm GNPs showed mild histological changes as mild fibrosis and edema in the renal medulla, and renal cortex with mild perivascular inflammatory cells infiltration, hypercellularity of a

Table 1. Semi-quantitative histopathological lesions score of all experimental groups.

	G1 (control)	G2 (10 nm GNPs)	G3 (20 nm GNPs)	G4 (50 nm GNPs)	G5 (Qur only)	G6 (10 nm GNPs + Qur)
Hypercellularity of renal glomeruli	–	++	++	+	–	+
Cloudy swelling of renal tubules lining epithelium	–	+++	++	+	–	–
Hemorrhage of renal cortex and medulla	–	+++	++	+	–	–
Congestion of renal blood vessels	–	+++	++	+	–	–
Perivascular inflammatory cells infiltration	–	+++	++	+	–	–
Inter-tubular edema	–	+++	++	+	–	–
Vascular endotheliosis	–	+++	++	+	–	–
Perivascular fibrosis	–	+++	++	+	–	–
Atrophy of some glomeruli and renal tubules	–	++	++	+	–	–
Glycogen deposition	–	+++	++	–	–	+
Casts depositions of renal tubules, mainly cellular casts	–	+++	+	–	–	–
Hemosiderosis	–	+++	++	–	–	–
Cystic dilatation	–	+++	++	+	–	+

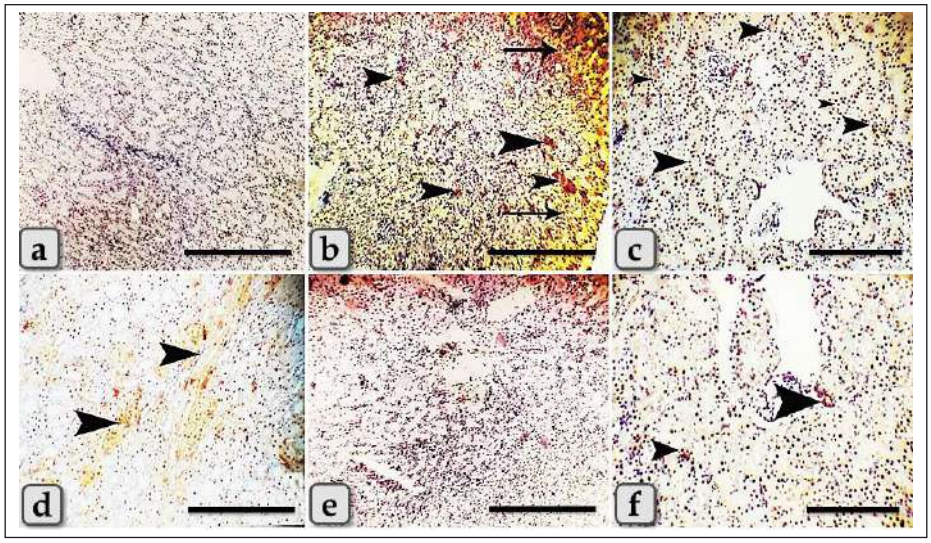

Fig. 5. A photomicrographs of the immunohistochemical stained kidney sections against anti-caspase-3 antibody of G1 (a) control group and G2 (b), G3 (c), G4 (d) those injected intraperitoneally with 10, 20, 50 nm GNPs consequently, G5 (e) that treated with Qur-only, and G6 (f); Qur + 10 nm GNPs showing, (a) negative expression with anti-caspase-3 antibody. (b) Limited distribution of strong expression (arrows head) with severe positive peripheral expressions for caspase-3 (arrows). (c) Minimal focal strong positive expressions for caspase-3(arrows head) scattered randomly. (d) Focal mild expression for caspase-3 (arrows head). (e) Negative expression for caspase-3. (f) Moderate positive cellular expressions for caspase-3 (arrowhead) Scale bars: All = 600 µm except, (c and f) = 200 µm.

few glomeruli with focal cloudy swelling of some renal epithelium. These results are in parallelism with Yahyaei *et al*. (2019) who assumed that even at very high concentrations, 50 nm GNPs caused only minor alterations in the vital organs of rats especially in the kidney that revealed a localized reduction in glomeruli.

There was no outward sign of damage to the renal tubes, but only interstitial hyperemia was present.

G6; Qur + 10 nm GNPs showed normal renal cortex and medulla but with slight histological changes as slight hypercellularity of some renal epithelium**,** and mild intratubular glycogen deposits. In addition, at the level of renal functional parameters, Qur treated group showed a good impact and recorded a significant decrease in all values compared to G2. These findings were indicating that Qur has more potent cytoprotective, anti-inflammatory, and anti-apoptotic effects and has a significant mitigating role against the nephrotoxicity of the GNPs.

Gholampour and Saki (2019) also supported our results and revealed the reduced histological damage in the kidney was evidence that Qur protected the renal tissue and cells against toxicity. In addition, Das *et al*. (2020) clarified that Qur therapy decreased the histological changes, stabilized plasma biomarkers, suppressed oxidative stress, reduced apoptosis, and provided greater protection against NPs-induced nephrotoxicity rats.

Conclusion

The size of GNPs is pivotal in their pathological effect on renal tissues where the small-sized GNPs; 10 nm have more potent cytotoxic, inflammatory, and apoptotic effects rather than the larger ones. Otherwise, Qur clarified a significant mitigating role against the nephrotoxicity of the GNPs.

Author contribution

Conceptualization: WG. Data curation, investigation: WG. Methodology: WG, AA, FA. Histopathological examination—images analyze: WG, FA. Writing-iriginal draft: WG, FA. Review and editing: WG, FA, SE. All the authors read and approved the final version of the manuscript.

Funding

This work did not receive any grant from any commercial, public, or not-for-profit sectors.

Conflict of interest

The authors declare that they have no competing interests.

References

Abdelhalim, M.A.K. and Jarrar, B.M. 2011. Gold nanoparticles induced cloudy swelling to hydronic degeneration, cytoplasmic hyaline vacuolation, polymorphism, binucleation, karyopyknotic, karyolysis, karyorrhexis and necrosis in the liver. Lipids Health Dis. 10, 16.

Abdelhalim, M.A.K. and Jarrar, B.M. 2012. Histological alterations in the liver of rats induced by different gold nanoparticle sizes, doses and exposure duration. J. Nanobiotechnol. 10, 1–9.

Abdelhalim, M.A.K., Qaid, H.A., Al-Mohy, Y. and Al-Ayed, M. S. 2018. Effects of quercetin and arginine on the nephrotoxicity and lipid peroxidation induced by gold nanoparticles *in vivo*. Int. J. Nanomed. 13, 7765.

Abdelhalim, M.A.K., Qaid, H.A., Al-Mohy, Y. and Ghannam, M.M. 2020. The protective roles of vitamin E and α-lipoic acid against nephrotoxicity, lipid peroxidation, and inflammatory damage induced by gold nanoparticles. Int. J. Nanomed. 15, 729–734.

Aguirre, L., Arias, N., Macarulla, M.T., Gracia, A. and Portillo, M.P. 2011. Beneficial effects of quercetin on obesity and diabetes. Open Nutraceuticals J. 4, 189–198.

Alasmari, A.F. 2021. Cardioprotective and nephroprotective effects of quercetin against different toxic agents. Eur. Rev. Med. Pharmacol. Sci. 25, 7425–7439.

Baghel, S.S., Shrivastava, N., Baghel, R.S., Agrawal, P. and Rajput, S. 2012. A review of quercetin: antioxidant and anticancer properties. WJPPS 1, 1460–160.

Bayda, S., Adeel, M., Tuccinardi, T., Cordani, M. and Rizzolio, F. 2019. The history of nanoscience and nanotechnology: from chemical–physical applications to nanomedicine. Molecules 25, 112.

Cai, W., Gao, T., Hong, H. and Sun, J. 2008. Applications of gold nanoparticles in cancer nanotechnology. Nanotechnol. Sci. Appl. 1, 17.

Chen, H., Dorrigan, A., Saad, S., Hare, D.J., Cortie, M.B. and Valenzuela, S.M. 2013. *In vivo* study of spherical gold nanoparticles: inflammatory effects and distribution in mice. PLoS One 8, 1–8.

Dabeek, W.M. and Marra, M.V. 2019. Dietary quercetin and kaempferol: bioavailability and potential cardiovascular-related bioactivity in humans. Nutrients 11, 2288.

Das, S.S., Verma, P.R.P., Kar, S. and Singh, S.K. 2020. Quercetin-loaded nanomedicine as oncotherapy. In Nanomedicine for bioactives. Singapore: Springer Singapore, pp: 155–183.

Doudi, M. and Setorki, M. 2014. The effect of gold nanoparticle on renal function in rats. Nanomed. J. 1(3), 171–179.

Fadia, B.S., Mokhtari-Soulimane, N., Meriem, B., Wacila, N., Zouleykha, B., Karima, R. and Thorat, N.D. 2022. Histological injury to rat brain, liver, and kidneys by gold nanoparticles is dose-dependent. ACS Omega 7, 20656–20665.

Falagan, L.P., Grzincic, E.M. and Murphy, C.J. 2016. One low-dose exposure of gold nanoparticles induces long-term changes in human cells. Proc. Natl. Acad. Sci. USA. 113, 13318–13323.

Gheorghe, D.C., Niculescu, A.G., Bîrcă, A.C. and Grumezescu, A.M. 2021. Nanoparticles for the treatment of inner ear infections. Nanomaterials 11, 1311.

Gholampour, F. and Saki, N. 2019. Hepatic and renal protective effects of quercetin in ferrous sulfate-induced toxicity. Gen. Physiol. 38, 1, 27–38.

Ghonimi, W.A.M., Alferah, M.A.Z., Dahran, N. and El-Shetry, E.S. 2022. Hepatic and renal toxicity following the injection of copper oxide nanoparticles (CuO NPs) in mature male Westar rats: histochemical and caspase 3 immunohistochemical reactivities. Environ. Sci. Pollut. Res. 29, 81923–81937.

Hatahet, T., Morille, M., Shamseddin, A., Aubert-Pouëssel, A., Devoisselle, J. and Bégu, S. 2017. Dermal quercetin lipid nanocapsules: influence of the formulation on antioxidant activity and cellular protection against hydrogen peroxide. Int. J. Pharm. 518, 167–176.

Ibrahim, K.E., Al-Mutary, M.G., Bakhiet, A.O. and Khan, H.A. 2018. Histopathology of the liver, kidney, and spleen of mice exposed to gold nanoparticles. Molecules 23, 1848.

Jarrar, B.M. and Alferah, M.A. 2014. Renal histological alterations induced by 10 nm gold nanoparticles toxicity in relation with the time of exposure. Lat. Am. J. Pharm. 33(5), 725–730.

Jeevanandam, J., Barhoum, A., Chan, Y.S., Dufresne, A. and Danquah, M.K. 2018. Review on nanoparticles and nanostructured materials: history, sources, toxicity and regulations. Beilstein J. Nanotechnol. 9, 1050–1074.

Jellin, J.M., Batz, F. and Hitchens, K. 2003. Pharmacist's letter/prescriber's letter. Stockton, CA: Natural Medicines Comprehensive, Database Therapeutic Research Faculty, pp: 1100–1101.

Jiang, Y., Wang, M., Hardie, J., Tonga, G.Y., Ray, M., Xu, Q. and Rotello, V.M. 2016. Chemically engineered nanoparticle-protein interface for real-time cellular oxidative stress monitoring. Small 12, 3775–3779.

Kong, F.Y., Zhang, J.W., Li, R.F., Wang, Z.X., Wang, W.J. and Wang, W. 2017. Unique roles of gold nanoparticles in drug delivery, targeting and imaging applications. Molecules 22, 1445.

Kumar, A., Zhang, X. and Liang, X. J. 2013. Gold nanoparticles: emerging paradigm for targeted drug delivery system. Biotechnol. Adv. 31, 593–606.

Orabi, S.H., Mansour, D.A., Fathalla, S.I., Gadallah, S.M., Gamal Eldin A.A. and Abdoon, A.S.A. 2022. Effects of administration of 10 nm or 50 nm gold nanoparticles (AuNPs) on blood profile, liver and kidney functions in male albino rats. IJBB. 57, 486-493.

Polak, J.M. and Noorden, V. 1997. Introduction to immunocytochemistry. In: BIOS, 2nd ed. Oxford, UK: Scientific Publishers.

Suvarna, S.K., Layton, C. and Bancroft, J.D. 2018. Bancroft's theory and practice of histological techniques, 8th ed. New York, NY/London, UK: Churchill Livingstone, pp: 83–92.

Wang, X.F., Zhu, M.T. and Li, J.Y. 2012. Biomedical effects and nanosafety of engineered nanomaterials: recent progress. Chin. J. Chem. 30, 1931–1947.

Xu, D., Hu, M.J., Wang, Y.Q. and Cui, Y.L. 2019. Antioxidant activities of quercetin and its complexes for medicinal application. Molecules 24, 1123.

Xu, M.X., Wang, M. and Yang, W.W. 2017. Gold-quercetin nanoparticles prevent metabolic endotoxemia-induced kidney injury by regulating TLR4/NF-κB signaling and Nrf2 pathway in high fat diet fed mice. Int. J. Nanomed. 12, 327–345.

Yahyaei, B., Nouri, M., Bakherad, S., Hassani, M. and Pourali, P. 2019. Effects of biologically produced gold nanoparticles: toxicity assessment in different rat organs after intraperitoneal injection. AMB Express. 9(1), 1–12.

Yamashita, M. 2021. Auranofin: past to present and repurposing. Int. Immunopharmacol. 101(pt B), 108272.

Yang, H., Song, Y., Liang, Y. and Li, R. 2018. Quercetin treatment improves renal function and protects the kidney in a rat model of adenine-induced chronic kidney disease. Med. Sci. Monit. 24, 4760–4766.